Received: 3 March 2021 | Accepted: 1 February 2022

DOI: 10.1111/1365-2435.14029

Functional Ecology | BRITISH ECOLOGICAL SOCIETY

RESEARCH ARTICLE

Do leaf nitrogen resorption dynamics align with the slow-fast continuum? A test at the intraspecific level

Kevin Sartori[1] | Cyrille Violle[1] | Denis Vile[2] | François Vasseur[1,2] | Pierre de Villemereuil[3] | Justine Bresson[1] | Lauren Gillespie[1] | Leila Rose Fletcher[4] | Lawren Sack[4] | Elena Kazakou[1,5]

[1]CEFE, Univ Montpellier, CNRS, EPHE, IRD, Montpellier, France

[2]LEPSE, Univ Montpellier, INRAE, Institut Agro, Montpellier, France

[3]Institut de Systématique, Évolution, Biodiversité (ISYEB), École Pratique des Hautes Études PSL, MNHN, CNRS, Sorbonne Université, Université des Antilles, Paris, France

[4]University of California, Los Angeles, CA, USA

[5]Univ Montpellier, Institut Agro, Montpellier SupAgro, Montpellier, France

Correspondence
Kevin Sartori
Email: kevinfrsartori@gmail.com

Funding information
H2020 European Research Council, Grant/Award Number: ERC-StG-2014-639706-CONSTRAINTS

Handing Editor: Carlos Perez Carmona

Abstract

1. The links between internal nitrogen recycling through the process of resorption from senescing leaves, whole-plant resource-use strategies and performance remain elusive. Indeed, tests of such potential linkages are hampered by the classical evaluation of plant nitrogen resorption efficiency (RE_N) based on 'snapshots' of leaf nitrogen concentration from adult and senescent leaves.
2. We significantly increased the resolution for measuring leaf nitrogen resorption by non-destructively tracking time courses of nitrogen concentration in leaves of 137 natural *Arabidopsis thaliana* genotypes native to a wide range of climates across Europe, grown in a greenhouse. In addition to the classical measurement of resorption efficiency, we computed the relative maximum resorption rate of nitrogen (RR_N), that is, the amount of nitrogen remobilized by a leaf per unit time and per unit nitrogen, together with slow–fast syndrome traits at the leaf and whole-plant levels.
3. Across genotypes, high rates and efficiencies of nitrogen resorption were associated with low specific leaf area and late flowering. The RR_N showed significant heritability, genetic associations and was negatively correlated with the mean annual temperature of the native populations. By contrast, despite the evidence of a correlation with temperature, RE_N showed lower heritability and no evidence of genetic association, questioning the mechanisms of nitrogen resorption.
4. Overall, our results suggest a much stronger adaptive role for leaf nitrogen resorption than previously uncovered.

KEYWORDS
Arabidopsis thaliana, association genetics, leaf nitrogen, population genetics, resorption, resource-use strategies

1 | INTRODUCTION

Leaf nitrogen resorption plays a major role in the plant nutrient budget, remobilizing and relocating nitrogen from senescing organs to surviving tissues (Killingbeck, 1986). This process increases nitrogen mean residence time, enabling plants to mitigate the nitrogen limitation that exists in most natural ecosystems (Aerts & Chapin, 1999; Berendse & Aerts, 1987). Despite the tremendous importance of nitrogen resorption for plant physiology and ecology, its role in leaf and plant resource-use strategies as well as its contribution to species local adaptation remains unresolved.

The search for global patterns in resource-use strategies in functional ecology has generally focused on trait variations during the 'green phase' of the leaf. The 'worldwide leaf economics spectrum' (LES) describes a pervasive syndrome of leaf traits going from short-lived to fast-lived leaves (Salguero-Gómez, 2017; Wright et al., 2004). On one extreme, species produce short-lived leaves that exhibit traits related to rapid metabolism (high photosynthetic rate, large area per unit leaf mass (specific leaf area [SLA]) and high nutrient concentrations), and on the other extreme, species produce long-lived leaves that exhibit a slow metabolism, low SLA and low nutrient concentration. Given that nitrogen mean residence time is a determinant of operational nitrogen concentration (Aerts & Chapin, 1999), one might thus expect that leaf resource-use strategies, and thus, LES traits would be associated with nitrogen resorption (Freschet et al., 2010; Kazakou et al., 2007; Rea et al., 2018). However, the few studies examining the coupling between nitrogen resorption and LES across species did not show consistent patterns (Achat et al., 2018; Campanella & Bertiller, 2011; Freschet et al., 2010; Kazakou et al., 2007; Rea et al., 2018; Yuan & Chen, 2010). We see several limitations that could lead to this pattern. First, nitrogen resorption is a complex, dynamic and multifaceted molecular choreography barely captured by 'snapshots' of leaf trait measurements (Harper & Sellek, 1987; Reich et al., 1991) as it has been recommended in comparative ecology (Aerts & Chapin, 1999). Second, little is known about the asynchrony of traits dynamics such as leaf area (LA), dry mass (DM), photosynthetic ability while leaves are senescing (Pantin et al., 2012) which can blur the trait–resorption relationships. Finally, interspecific variation across other leaf traits and species-specific biochemical and biophysical determinants of nitrogen resorption might be a confounding factor in the LES traits–resorption efficiency relationship (Rea et al., 2018).

Traditional comparative approaches for measuring nitrogen resorption have focused on the proportion of nitrogen resorbed between the adult stage and the end of the leaf life cycle (namely resorption efficiency, RE_N) and the leaf nitrogen concentration (LNC) at the end of the leaf life cycle (namely nitrogen resorption proficiency; Aerts & Chapin, 1999). However, there are many ways to obtain comparable nitrogen resorption efficiencies. The dynamics of nitrogen resorption can be informative of the overall metabolic machinery of the leaf and provides a more comprehensive understanding of plants' nutrient-use strategies (Figure 1). The ecological importance of leaf resorption dynamics and how it affects resorption efficiency

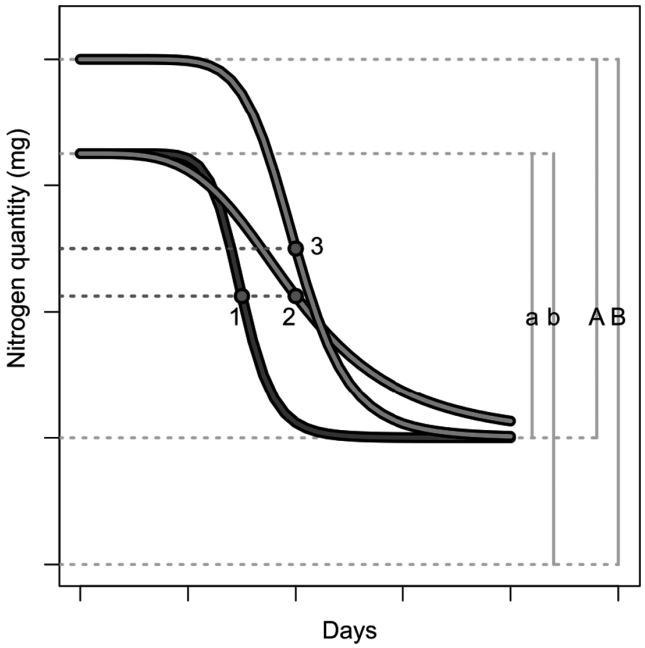

FIGURE 1 Expected leaf nitrogen dynamics for slow-growing (green) versus fast-growing (blue) plants. The figure represents the hypothetical dynamics at leaf end-of-life, as soon as leaf nitrogen quantity starts to decrease. Red dashed lines materialize the instantaneous N quantity value used to standardize the resorption slope measured at the maximum inflection of the curves (red dots). Case 1 represents the hypothetical leaf N dynamics of a fast-growing plant. Case 2 presents a lower rate of resorption due to a lower slope of N decrease. Case 3 presents a lower rate of resorption due to an overall higher leaf N content while the slope is similar to case 1. Solid grey lines materialize the nitrogen quantity resorbed (a and A), and the maximum nitrogen quantity (b and B) used to calculate the resorption efficiency as a/b (cases 1 and 2) and A/B (case 3). Resorption efficiency of case 3 is greater than cases 1 and 2

has been suggested in tree species comparisons (Niinemets & Tamm, 2005). However, the analysis suffers from complex leaf size and mass standardization since different leaves were sequentially destructed for the measurements. Non-destructive measurements are now possible using near-infrared spectroscopy (NIRS) that enables the estimation of material properties from light absorbance (Ecarnot et al., 2013) and can help monitor the temporal variation of LNC (Vilmus et al., 2014). We define the relative maximum resorption rate of nitrogen (RR_N) as the amount of nitrogen remobilized by a leaf per unit time and per leaf nitrogen quantity. We aim to assess the potential of a leaf to resorb nitrogen. To this end, we designed RR_N as a maximum and instantaneous resorption rate, by locating the maximum decrease in nitrogen quantity and dividing it by the instantaneous nitrogen quantity (Figure 1). In the literature, high metabolic rates and high nutrient concentration were associated with higher rates of nutrient resorption (Niinemets & Tamm, 2005; Osaki & Shinano, 2001). We thus expect RR_N to either be embedded by the leaf slow–fast metabolic syndrome due to phenotypic integration or constrained by slow–fast physiologic adaptations. In that respect,

slow-growing leaves should exhibit low RR_N over a long leaf life span, whereas fast-growing leaves should display high RR_N over a short period of time (Figure 1).

The leaf-level slow–fast trade-off may reflect a whole-plant slow–fast trade-off (Reich, 2014; Salguero-Gómez et al., 2016). Thus, species characterized by 'slow' LES traits would grow slowly, reach maturity later, live longer and more effectively conserve resources over their life span (conservative strategy). By contrast, species with 'fast' LES traits should grow faster, reach maturity earlier, have shorter life spans and more effectively acquire resources (acquisitive strategy). Several studies have been questioning the existence of a whole-plant syndrome by exploring trade-offs in different organs. For instance, some dimensions of the root trait syndrome were weakly correlated or orthogonal to the LES (Isaac et al., 2017; Tjoelker et al., 2005; Withington et al., 2006). Similarly, a wood trait syndrome might be preferentially driven by hydraulic trade-offs (Chave et al., 2009) and decorrelates from leaf slow–fast trade-offs as suggested by Baraloto et al. (2010). By contrast, empirical evidence of the connection between leaf-level and plant-level resource-use strategies has been supported by recent intraspecific studies (Sartori et al., 2019). Accordingly, and given its crucial role for seed production (Masclaux-Daubresse & Chardon, 2011), we hypothesize a strong influence of nitrogen resorption for plant-level resource-use and fitness. Moreover, nitrogen resorption might be advantageous under adverse conditions, when resources are missing, and thus correlate with the plant-level resource-use strategy. According to functional ecology and biogeography studies, species or genotypes with conservative trait values are better adapted to harsh environmental conditions (e.g. Borgy et al., 2017). Thus, we expect higher rates and lower efficiency of resorption for genotypes native to environments that are more favourable. Empirical tests of this assumption remain scarce and limited to local and site-specific studies. Yuan and Chen (2009) performed a meta-analysis, gathering resorption efficiencies across species distributed worldwide. The authors reported a significant decrease in nitrogen resorption efficiency with increasing temperature and precipitation. However, across the genus Helianthus, Rea et al. (2018) showed that species with higher resorption efficiency occupy warmer and wetter habitats. Diverging responses at different organization scales are expected to occur when measuring traits covariation across environments and species (Agrawal, 2020). The comparison of populations of a single species distributed along environmental gradients by using a common garden approach is now essential to test whether natural selection underlines a resorption–environment relationship.

Arabidopsis thaliana is a model species for not only genetic studies, but increasingly for ecological studies given its broad climatic range, and large variation in life-history traits (e.g. Brachi et al., 2012; Mitchell-Olds, 2001) and functional traits, notably those related to the LES (Sartori et al., 2019; Vasseur et al., 2018). *A. thaliana* is an herbaceous annual species with a large distribution spanning from the Mediterranean coast to Northern Sweden and across Asia. This distribution covers considerable variation of climatic conditions that are correlated with the genetic structure of *A. thaliana's* populations, suggesting underlying local adaptation (Lasky et al., 2012). The genetic determinism of the life cycle length, most often measured as the germination–flowering time (FT) interval, has been particularly well explored given its key role in *A. thaliana* adaptation to contrasting environments (e.g. Lovell et al., 2013; Mendez-Vigo et al., 2011; Schmalenbach et al., 2014). A recent study revealed that intraspecific variation of life-history traits and leaf economics traits such as leaf N:C through space and time is associated with environmental changes (DeLeo et al., 2020). Furthermore, studies uncovered common genetic bases for FT and LES traits (Vasseur et al., 2012), and evidenced that the differentiation of these traits is mediated by abiotic stresses (Vasseur et al., 2018). Substantial variability in resorption efficiency has been detected among a few genotypes (Masclaux-Daubresse & Chardon, 2011), reflecting variation in the genetic and metabolic pathways involved in proteolysis and transport of N-bearing molecules (Havé et al., 2017). However, the broader range of natural variability of nitrogen resorption requires assessment for a large panel of genotypes from contrasting environments and assessment of its role in plant fitness and species' local adaptation. We propose to merge molecular biology, population genetics and functional ecology to make the trait–fitness–environment linkage through the exploration of trait-to-genotype and genotype-to-environment linkages.

We quantified the phenotypic and environmental variation of nitrogen resorption and performed a genetic association study using common garden-grown ecotypes representing 137 *A. thaliana* populations sampled across the bulk of their native climate range. We hypothesized (1) strong variability in nitrogen resorption across ecotypes spanning this native climatic range, (2) that rate and efficiency of leaf nitrogen resorption are associated with the slow–fast trade-off, (3) that the natural variation of resorption traits has genetic bases that have been selected in contrasting environments.

2 | MATERIALS AND METHODS

2.1 | Plant material and growth conditions

We selected 153 natural genotypes from the 1001 GENOMES PROJECT list (Alonso-Blanco et al., 2016), maximizing the geographic distribution and variance of the life cycle duration of the *A. thaliana* populations selected (Sartori et al., 2019; Vasseur et al., 2018; Table S1). Pots (5 × 5 × 12 cm) were filled with a 1:1 mixture of sand and soil collected from the experimental field of the Centre d'Écologie Fonctionnelle et Évolutive (CEFE, Montpellier, France). This soil has a relatively low total nitrogen concentration (1.38 ± 0.11 mg/g; Kazakou et al., 2007). A layer of 2–3 mm of organic compost (Neuhaus N2) was added to the soil surface in each pot to improve germination and seedling survival. Seeds were sown on 8 and 9 December 2016 on the soil surface of the pots. Pots were placed in the dark at 8°C for 1 month to ensure seed vernalization and then placed in a greenhouse at 18/15°C day/night with a 12.5-hr photoperiod. Eight individual plants per genotype were randomly

placed, spaced apart in a checkerboard manner to avoid self-shading, on 44 trays split across four tables. Tables were rotated daily to reduce block effects within the greenhouse. Measurements started at the bolting stage, that is, apparition of the flowering bud, for each individual plant. At this moment, we marked the largest leaf fully exposed to light of each individual plant. Above-ground parts of four replicates per genotype were harvested at bolting and kept in deionized water at 4°C for one night before conducting destructive measurements (see below). The four remaining replicates were used to perform non-destructive measurements on the marked leaf until complete senescence of the leaf (see below). We used the FT, that is, the number of days from germination to opening of the first flower as a proxy of the individual life cycle length. Individuals presenting germination or growing issues, and early mortality were discarded from the analysis, and we kept the genotypes represented by at least three replicates in both destructive and non-destructive treatments (i.e. 137 genotypes).

2.2 | Destructive measurements

The marked leaf of each harvested individual was collected at bolting and placed in a test tube with deionized water for rehydration during 24 hr at 4°C. Marked leaves were then scanned to determine the LA (mm^2). Marked leaves were oven-dried at 70°C for 72 hr to determine the leaf DM (mg). SLA (m^2/kg) was calculated as the ratio between LA and leaf DM. A subset of 126 randomly selected dry leaves representative of 73 genotypes was ground individually to assess LNC (%) at bolting using the Pregl–Dumas method performed with a CHN elemental analyser (Flash EA1112 Series; Thermo Finnigan).

2.3 | Non-destructive measurements

Leaf area of the marked leaf of each tracked individual was determined every second day from pictures taken with a smartphone (Microsoft Lumia 540®) equipped with an 8 Mpx camera and a white plastic cube sticks on the flashlight as a light diffuser. Using an aluminium board, we made a small light box attached to the smartphone, designed to squeeze the leaves between a white support and a transparent piece of plastic (Figure S1). Images were calibrated and LA was determined using ImageJ (Schneider et al., 2012). Time course measurements of the marked leaf optical properties were performed using a near-infrared spectrometer (LabSpec 4; ASD Inc.). Light absorbance of leaf tissues was recorded every second day for the spectral region 350–2,500 nm near the tip and at one edge of the leaves avoiding the midrib. Data represent leaf light absorbance for 2,150 successive wavelengths, averaged for tip and edge (Figure S2). Marked leaves were harvested at complete senescence, that is, when the leaf tissues were completely dry. Every single tracked leaf reached its minimum N content before harvest. Every single tracked leaf was oven-dried in order to measure its DM and estimate a senescent-SLA thanks to the last measured surface. Leaves were then ground individually (459 leaves in total) to assess LNC (%) as described above.

2.4 | Leaf nitrogen dynamics

The diagrammatic representation for N time course estimation procedure is presented in Figure S3. Near-infrared methods are designed to estimate relative material properties such as concentrations since they record a signal intensity out of a constant sensor size. Estimating the total nitrogen quantity of a leaf as a whole and its time variation thus requires to track the LA through time and multiply it by the leaf nitrogen quantity per unit area (LNA). LNA is obtained by the ratio between LNC (nitrogen quantity per unit leaf mass) and SLA (LA per unit leaf mass). The first step was predicting SLA and LNC from spectral records. A total of 882 (585) standard destructive measures of SLA (LNC) from harvested 'green' and tracked senescent leaves were used to calibrate the predictive models. For each individual leaf, we computed the average spectrum from the tip and edge records. We checked the presence of outliers by computing a Mahalanobis distance on the coordinates of a principal component analysis (Whitfield et al., 1987) and removed any spectrum exceeding the 95th quantile of the distances (813 and 547 remaining spectra respectively). We performed locally weighted partial least square regressions (Zavala-Ortiz et al., 2020) using measured SLA or LNC as the predicted variable and the wavelength absorbances as the predictor variables. Details of the spectrum pretreatments, model parameter selection and cross-validation method can be found in Supporting Information. Accuracy of the models was high for both SLA and LNC: The correlation coefficients of the predicted versus measured values regression were higher than 0.97 (Figure S4). We used those models to predict SLA and LNC of the whole set of spectral records (5,623 spectra).

Data exploration suggested that temporal trajectories of SLA and LNC with leaf age followed a decreasing sigmoidal trend and LA followed a bell-shaped curve (Figure 2). We first smoothed each curve using the Hampel algorithm. It is a window-based algorithm used for time-series data smoothing. For each central value x, and k, a positive integer defining the widow size, it tests whether x deviates significantly from the median of the $x - k$ to $x + k$ values. If the test is significant, it attributes the median to x; otherwise, it leaves x as it is. We therefore fitted time course data using a decreasing logistic function for SLA and LNC (Equation 1) and a third-degree polynomial function for LA.

$$y = D + \frac{A}{1 + e^{C\times(x-x_0)}}. \quad (1)$$

We estimated the parameters D, A, C and x_0 by using a nonlinear least-squares method. The parameter D represents the lowest value of y, A the difference between the minimum and maximum value of y, x_0 the day when the y decrease is maximal and C is proportional

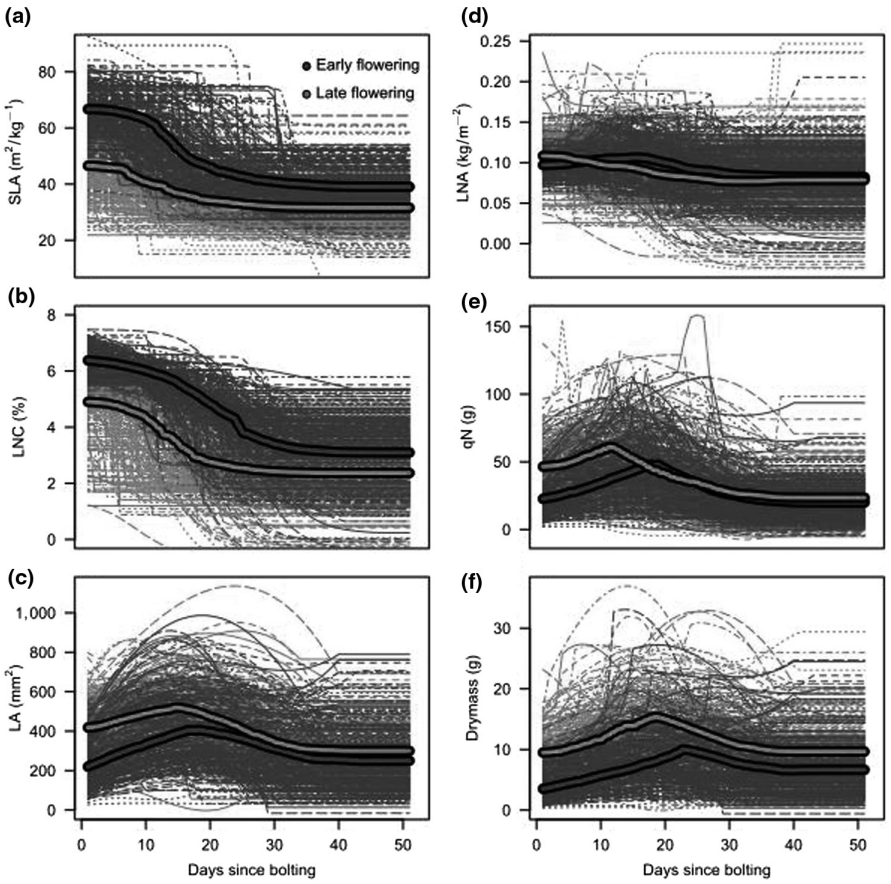

FIGURE 2 Observed temporal variability of leaf properties of early (blue) and late (green) flowering individuals of *Arabidopsis thaliana*. (a) SLA, specific leaf area (m^2/kg); (b) LNC, leaf nitrogen concentration (%); (c) area, leaf area (LA, mm^2); (d) LNA, leaf nitrogen per area (kg/m^2); (e) qN, nitrogen quantity (mg); and (f) DM, leaf dry mass (mg); as a function of days after flowering

to the slope of *y* decrease. We computed and saved the deviance of each individual fit for later outlier filtering. Time course of LNA, leaf nitrogen quantity and leaf DM were calculated as follows:

$$\mathrm{LNA} = \frac{\mathrm{LNC}}{\mathrm{SLA}}, \tag{2}$$

$$\mathrm{qN} = \mathrm{LNA} \times \mathrm{LA}, \tag{3}$$

$$\mathrm{DM} = \frac{\mathrm{LA}}{\mathrm{SLA}}. \tag{4}$$

We measured the relative maximum resorption rate of nitrogen (RR_N, mg day^{-1} mg^{-1}) for each tracked leaf as follows. We computed the local slopes from the first derivative value of qN dynamics at each time point. We then divided the maximum of the absolute slope values by the instantaneous nitrogen quantity of the leaf (Figure 1). Doing so, we account for the fact that higher rate of resorption might be a simple consequence of a larger leaf nitrogen stock.

$$\mathrm{RR_N} = \max\left\{\left|\frac{\partial \mathrm{qN}}{\partial t}\right| \div \mathrm{qN}_t\right\}. \tag{5}$$

We computed the nitrogen resorption efficiency (RE_N, %), that is, the proportion of total nitrogen resorbed by extracting the day and value of leaf maximum and minimum nitrogen quantity (dN_{max}, day; qN_{max}, mg, dN_{min}, day; qN_{min}, mg). Since a single leaf was tracked through time, there is no need for area and mass standardization (Heerwaarden et al., 2003), and RE_N can be directly calculated as:

$$\mathrm{RE_N} = \left(\mathrm{qN_{max}} - \mathrm{qN_{min}}\right) \div \mathrm{qN_{max}}. \tag{6}$$

Overall, the method we used to measure trait dynamic controls for dilution effects that may arise from leaf thickening, or from leaf mass and area increasing thanks to spectral pretreatments and precise daily mass and area tracking respectively. Thus, any change in leaf N status reflects leaf N in- and outfluxes and its synchronicity with development-related traits (e.g. LA and mass) can be assessed.

2.5 | Trait-to-genotype relationships

We performed the genome-wide association study (GWAS) of the efficiency and the rate of resorption using the GEMMA software (Zhou & Stephens, 2012). GWAS is based on the simple assumption that a single locus is associated with a trait variation if the mean trait values of two alleles are significantly different. GWAS screens the genotype for significant associations at the precision of single nucleotides, and along several million single nucleotides long genomes, from genotyping or sequencing data. The method uses the single-nucleotide polymorphisms (SNPs) as predictors of the traits in a linear mixed model. The population structure of the dataset can drastically influence the results and produce false positives.

For instance, if a new population is established after a colonization event, every allele inherited from, and specific to, the founder individuals will be significantly associated with any trait that distinguishes the historic population from the new population. GWAS' models use genetic correlation matrices to overcome this limitation. The results are usually represented in the form of a Manhattan plot that displays the significance of each single nucleotide–phenotype association along the genome, and candidate loci are filtered out from a Bonferroni significance threshold. From the genetic data available on the 1001 genomes project website (1001genomes.org), we excluded all variants with more than two possible alleles and all variants with a minor allele frequency lower than 0.05% (1,899,962 variants pass filters). Because we expect complex processes such as resorption to be polygenic and driven by small but numerous genetic locus effects, we used a local score approach to filter out SNPs associated with the traits (Bonhomme et al., 2019). Rather than using a simple significance threshold, the method computes a cumulative significance signal from contiguous SNPs. It has the advantage to consider the local linkage disequilibrium and exclude false positives characterized by a lack of surrounding association peak. A threshold is defined based on the initial GWAS *p*-value distribution and highlights loci significantly associated with the phenotype, namely quantitative trait loci (QTL). Using the Arabidopsis Information Resource database (www.arabidopsis.org), we extracted the list and functions of genes carried by the QTLs.

2.6 | Environment–to-genotype relationships

We predicted the phenotype of the whole set of *A. thaliana* accessions sequenced by the 1001 genome consortium. To this aim, we first run a Bayesian Sparse Linear Mixed Model (BSLMM) which computes both the overall proportion of phenotypic variance explained by the genotype (additive heritability) and estimates the individual effect size of each SNP on the phenotype (Zhou et al., 2013). We then used those estimates to predict the phenotype (RRN, REN) of the accessions that we did not measure. We used the collecting site coordinates of the accessions to extract their local environmental conditions—mean annual temperature (MAT) and mean annual precipitation (MAP)—from the CHELSA database (http://chelsa-climate.org/). We excluded from the analysis the 137 measured genotypes and 24 genotypes originating from sites encountering the levels of temperature and precipitation being out of the ranges of our sampled genotypes' sites (961 remaining genotypes). We assessed the strength and type of selection acting on the QTL identified by the GWAS by computing Weir and Cockerham F_{ST} indices (Weir & Cockerham, 1984). F_{ST} compares the between-population to the within-population genetic variance. When disruptive selection favours a specific allele in a specific population, the between-population variance is higher than the within-population variance and the F_{ST} index tends to 1. Under neutrality or stabilizing selection, F_{ST} index tends to 0. For significance, we compared the QTL F_{ST} to the mean F_{ST} computed on the whole chromosome they belong to. We used the genetic data described above for the whole set of genotypes from the 1001 genome initiative. We used as populations the large regional populations defined by Alonso Blanco et al. (2016).

2.7 | Statistical analyses

All statistical analyses but genetic analyses were performed using the R software (R Core Team, 2019, version 4.0.0).

The chemometric analyses were performed using the *rchemo* package (https://github.com/mlesnoff/rchemo) and we used the predictive model described by Lesnoff et al. (2020).

For better visualization, the overall patterns of trait dynamics were computed by using the *klmShape* package (Genolini et al., 2016).

We calculated trait genotype means by estimating the marginal means of the variables from linear mixed models including the genotype identity as a random effect and the experimental trays as fixed effects. The models were performed with the *lme* function from the *nlme* package, and the marginal means were computed with the *emmeans* function from the *emmeans* package (Searle et al., 1980).

Mean comparisons were performed using a Student's *t*-test with the *t.test* function. While testing the trait–trait relationships, we performed the Breusch–Pagan test against heteroscedasticity using the *bptest* function of the *lmtest* package and when significant, we performed the regression by using *lmrob* function from the *robustbase* package. Given the importance of the life cycle length in driving adaptive strategies in *A. thaliana*, we analysed the RR_N-SLA and RE_N-SLA relationships by controlling for the FT using partial correlations performed using the *ppcor* R package (Kim, 2015).

Genome data filtering was performed using the Plink software (Purcell et al., 2007); GWAS, BSLMM, relatedness matrices, broad sense heritability and phenotype prediction were computed using the GEMMA software (Zhou & Stephens, 2012; Zhou et al., 2013). F_{ST}-weighted indices were computed using the vcftools software (Danecek et al., 2011).

3 | RESULTS

3.1 | Leaf trait dynamics

Figure 2 shows the leaf trait dynamics of the whole set of tracked individuals. For a more informative representation, we split the dataset into two; early and late flowering, according to the individual date of flowering (less or more than the median FT respectively). We then computed the average dynamics for each group in order to help visualize the trends. Between individuals, maximum LA varied from 45.7 to 1,184 mm^2. On average (±*SE*), the marked leaves reached their maximum area 15.4 ± 10.8 days after bolting. LA decreased until complete senescence, following a bell-shaped curve. Between individuals, maximum SLA and LNC values ranged from 21.9 to 93.3 m^2/kg and from 1.2% to 7.5% respectively. SLA and LNC reached their maximum values significantly earlier than LA

(both $p < 0.01$) and then decreased following a sigmoidal curve. The N peak occurred on average 10.7 ± 7.8 days after bolting and varied from 3.6 to 158.6 mg. The N peak occurred significantly earlier than the LA peak ($p < 0.01$). The maximum inflection of qN dynamics (where RR_N is measured) occurred significantly later than the LA peak ($p < 0.01$) and on average 18.9 ± 11.4 days after bolting. Finally, the peak of leaf DM occurred significantly later than maximum LA ($p < 0.01$) and on average 18.6 ± 11.1 days after bolting.

3.2 | Trait variability and heritability

N resorption efficiency (mean $RE_N = 63.1 \pm 21.8\%$) and resorption rate (mean $RR_N = 0.20 \pm 0.23$ mg day^{-1} mg^{-1}) displayed significant variation among natural genotypes and had narrow heritabilities (h^2) of 0.35 and 0.43 respectively. Traits related to the structure and composition of the leaves were highly heritable: DM (13.7 ± 7.2 mg; $h^2 = 0.70$), LA (486.7 ± 177.9 mm^2; $h^2 = 0.58$), SLA (57.3 ± 14. mm^2/mg; $h^2 = 0.99$), LNC (5.7 ± 1.2%, h^2 ~0.99) and maximum nitrogen quantity (58 ± 27.2 mg, $h^2 = 0.47$). FT was also a highly heritable trait (52.6 ± 13.9 day, h^2 ~0.99). For a chart of a trait correlation matrix, see Figure S5.

3.3 | Relationships between nitrogen resorption and slow–fast traits

Across ecotypes, RR_N was negatively associated with SLA ($r = -0.38$, $p < 0.01$) and positively associated with FT ($r = 0.39$, $p < 0.01$; Figure 3a,b). The negative relationship of RR_N with SLA was not independent of FT (partial correlation r ~0, $p = 0.57$). Furthermore, RE_N was negatively associated with SLA ($r = -0.22$, $p < 0.05$) and positively associated with FT ($r = 0.23$, $p < 0.05$; Figure 3c,d), and the relationship of RE_N and SLA was also not independent of FT (partial correlation r ~0, $p = 0.74$).

3.4 | Relationships between nitrogen resorption and climate

RR_N was negatively associated with increasing temperature ($r = -0.29$, $p < 0.001$) and was uncorrelated with the average precipitation, measured at the genotype collecting sites (Figure 4a,b). RE_N was negatively associated, to a lesser extent, with site temperature ($r = -0.28$, $p < 0.05$) and uncorrelated with site precipitation (Figure 4c,d). Lower significance of the correlation between RE_N and MAT might be the result of a triangular relationship, supported by the heteroscedasticity of the residuals (p ~0.05) and the nearly significant slope difference between the 0.05 and 0.95 quantile regressions (p ~0.069).

Resorption traits-to-genotype relationships.

The GWAS revealed two loci significantly associated with RR_N located on chromosomes 1 and 4 (Figure 5, $p < 0.01$), and two significant loci on chromosome 5 (Figure S5, $p < 0.05$). The first locus (Chromosome 1, from 4266820 to 4272775 bp) contains two genes, the *A. thaliana* Copper Chaperone for SOD1 (ATCCS) and a hypothetical protein (AT1G12530). The ATCCS gene activity is localized to the

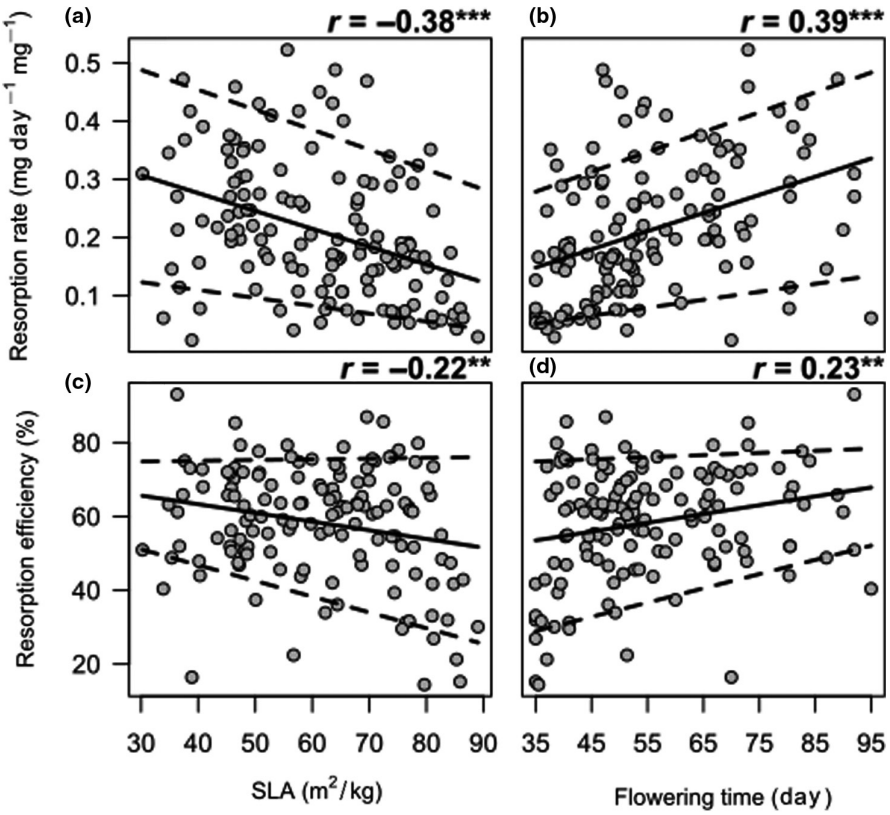

FIGURE 3 Relationships between nitrogen resorption, specific leaf area (SLA) and flowering time across natural genotypes of *Arabidopsis thaliana*. Each dot represents the average trait value of a natural genotype (grey circles; $n = 137$). Solid lines represent significant linear relationships at $p < 0.05$. Dashed lines represent quantile regressions for the 0.95 and 0.05 quantiles. Correlation coefficients r of a linear model are reported for each relationship together with their significance (***$p < 0.001$; **$p < 0.01$; *$p < 0.05$; NS, non significant)

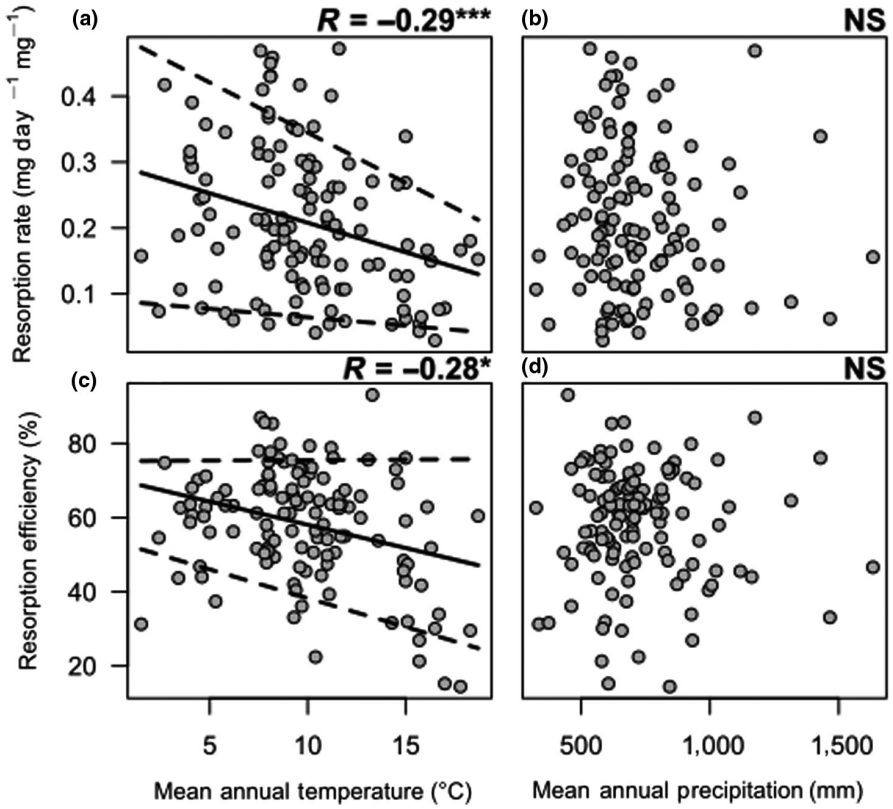

FIGURE 4 Relationships between the resorption traits and the main biogeography's climatic variables measured at the genotype collecting sites. Each dot represents the average value of a natural genotype ($n = 137$) of (a, b) resorption rate and (c, d) resorption efficiency as a function of the average annual temperature (a, c) and the average annual precipitation (b, d). Solid lines represent significant linear relationships at $p < 0.05$. Dashed lines represent quantile regressions for the 0.95 and 0.05 quantiles. Correlation coefficients r of a linear model are reported together with their significance (***$p < 0.001$; **$p < 0.01$; *$p < 0.05$; NS, non significant)

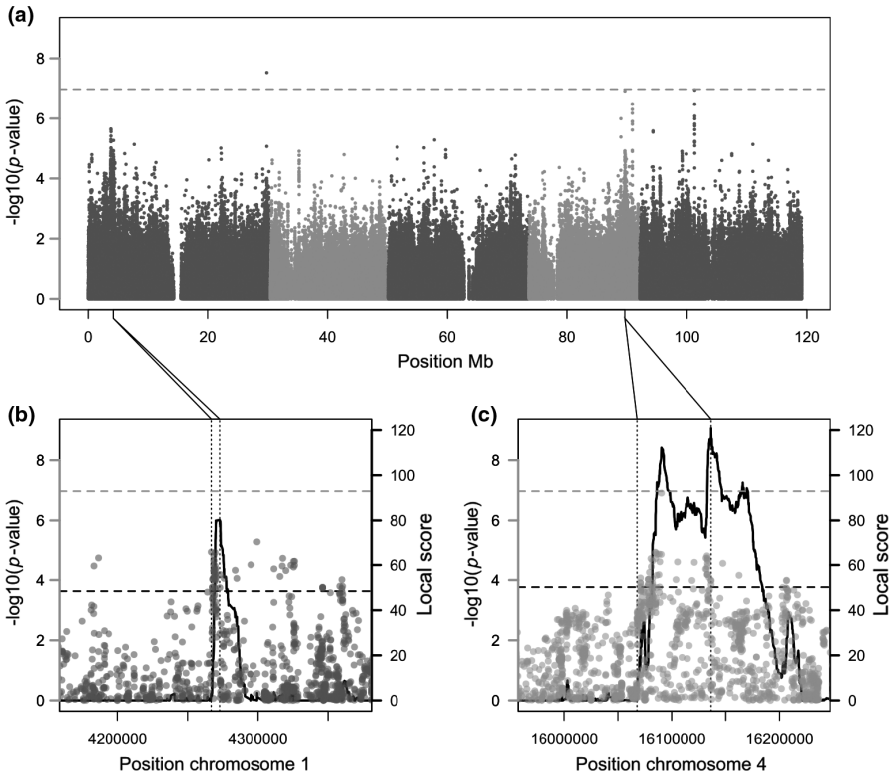

FIGURE 5 The polymorphism of two short sequences of *Arabidopsis thaliana* genome is associated with the resorption rate variation. Panels are Manhattan plots, (a) representing the strength of the association between each single-nucleotide (grey dots) polymorphism and the resorption rate variation, and (b, c) representing the local score of significance for the two significant loci in chromosomes 1 and 4. Green dashed lines represent the significance threshold calculated with the Bonferroni method. The horizontal dashed black lines delineate the loci detected with the local score calculated in either direction. Dots' shades of green delineate the five *A. thaliana* chromosomes

chloroplast and is upregulated in response to senescence (Berardini et al., 2015). SOD1 encodes a cytosolic copper/zinc superoxide dismutase CSD1 that can detoxify superoxide radicals. The large locus observed on chromosome 4 (from 16067742 to 16136370 bp) contains a cluster of 24 genes that can be involved in wounding, stress tolerance and, for many of them, have an activity localized to the chloroplast (Table S2). Consistent with its weaker heritability, we found no significant genetic association with RE_N (Figure S6).

3.5 | Genotype-to-environment relationships

The predicted RR_N and RE_N covered a shorter value range (0.21 ± 0.03 mg day^{-1} mg^{-1} and 58.65 ± 4.78% respectively) than measured RR_N and RE_N. Both traits were significantly and negatively correlated with MAT (r_{RRN} = −0.52; r_{REN} = −0.55, both $p < 0.001$; Figure 6a,b), and uncorrelated with MAP. Across the whole 1001 genome set of 1,135 *A. thaliana* accessions, the ATCCS gene contains 151 polymorphic sites and was best clustered with $K = 2$ ($N_{Allele1}$ = 835, $N_{Allele2}$ = 263; $CVerror_{K=1}$ = 1.03; $CVerror_{K=2}$ = 0.12; $CVerror_{K=3}$ = 0.15). The two ATCCS alleles originated from sites that significantly differ from temperature ($mean_{Allele1}$ = 10.42; $mean_{Allele2}$ = 7.80; $p_{Ttest} < 0.001$, Figure 6c) and latitude ($mean_{Allele1}$ = 45.80; $mean_{Allele2}$ = 55.70; $p_{Ttest} < 0.001$). The average Weir & Cockerham F_{ST} estimate along the ATCCS gene was 0.46 ± 0.23 and was about 0.19 across the first chromosome. The average Weir & Cockerham F_{ST} estimate along the QTL4 was 0.27 ± 0.13 and was about 0.20 across the fourth chromosome. We can conclude that ATCCS is significantly differentiated between populations compared to the average first chromosome signal, while QTL4 is not.

4 | DISCUSSION

Historically, plant nutrient resorption is commonly evaluated through the outcome of the resorption process, that is, resorption efficiency (Killingbeck, 1986). This approach meets a need to establish the economic record of leaves (Bloom et al., 1985; Wright et al., 2004). Consistent with previous interspecific comparisons, resorption efficiency in *A. thaliana* was high on average (>60%; Kazakou et al., 2007) and showed a medium value of broad-sense heritability (~30%; e.g. Mikola et al., 2018). In addition, our results show a lack of significant trait-to-genotype association, heritability and adaptive value along environmental gradients for the resorption efficiency. Together, these findings suggest that a substantial efficiency of resorption is invariably favoured across plant strategies and environments. An investigation of the role of stabilizing selection in shaping resorption efficiency patterns would be needed to test this conjecture. Using an innovative method based on the near-infrared absorbance of leaf tissues (Vilmus et al., 2014), we tracked daily changes in nitrogen quantity in living leaves. Using this dataset, we were able to measure the maximum rate of nitrogen content decrease during leaf senescence. To our knowledge, this is the first time such a relative and maximum resorption rate of nitrogen has been reported. The resorption rate was highly variable (16-fold among genotypes), heritable (broad-sense heritability = 45%) and strongly correlated with leaf and plant level trait syndromes and this variation correlated with environmental gradients. But what really makes the difference compared to the resorption efficiency is the strong genetic association detected in our data. The existence of two haplotypes segregating in populations that differ by climatic variables suggests that disruptive selection maintains genetic and phenotypic variability associated with the resorption rate of nitrogen. In this context, the resorption rate of nitrogen proves to be a promising candidate for describing differences in resorption strategies between genotypes.

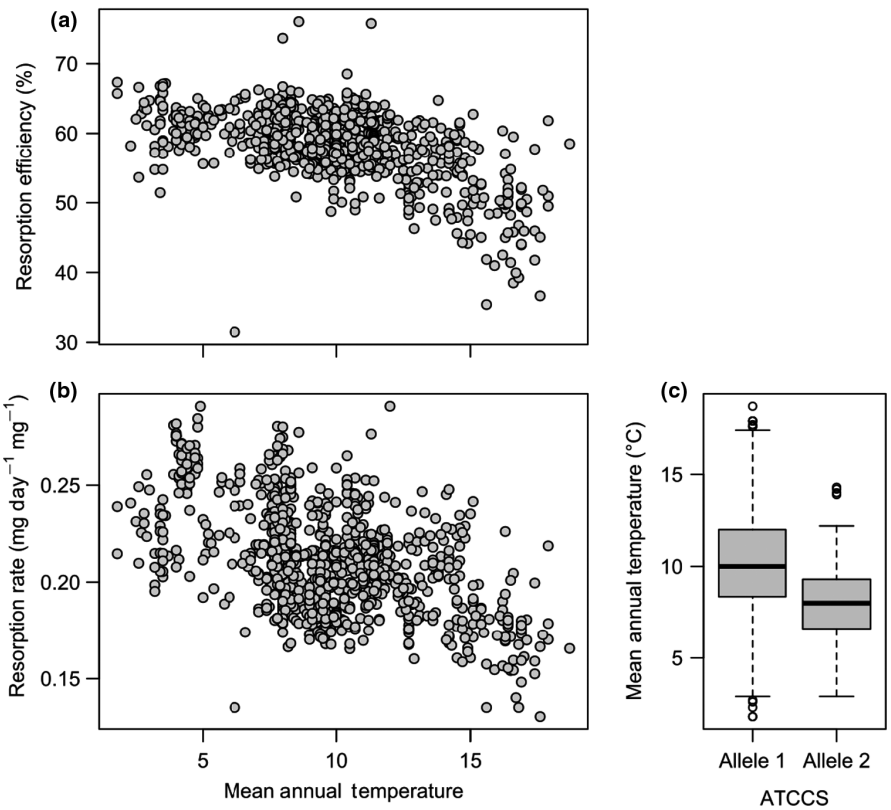

FIGURE 6 Relationships between the mean annual temperature measured at the collecting sites and the predicted resorption traits of 961 *Arabidopsis thaliana* natural genotypes. (a) Resorption rate and (b) resorption efficiency as a function of the mean annual temperature, (c) boxplot representing the association between the mean annual temperature and the *A. thaliana* Copper Chaperone for SOD1 (ATCCS) alleles favoured at the genotype collecting sites

Furthermore, we discuss the potential role of the resorption rate of nitrogen for plant adaptation to contrasted environments. Overall, our findings suggest a need for studies exploring the genetic, physiological and morphological variations responsible for time course variations in nitrogen quantity.

The daily monitoring of multiple leaf traits provides new insights about changes in leaf properties during leaf senescence. Previous studies reported that in *A. thaliana*, leaf senescence begins as soon as or after leaves reach their full adult size and maximum sugar content value (Diaz et al., 2005, 2008; Himelblau & Amasino, 2001). These studies highlighted that nitrogen, starch, protein and chlorophyll contents decrease, and leaf yellowing starts as soon as leaves reach full expansion. Our results do not support this assertion; among the 137 natural *A. thaliana* genotypes studied, LNC started to decrease on average a few days before leaves were fully expanded, suggesting that first signs of senescence occur before complete leaf maturity. This unexpected pattern may arise for two reasons: (1) the leaf N status does not reflect the photosynthetic maturity of the leaf; (2) morphological and physiological leaf maturity are asynchronous. First, studies showed that leaves build up N reserves at their juvenile stage and N remobilization is triggered by transition to reproductive stage (Santiago & Tegeder, 2017). Thus, the initial decrease in leaf N quantity during leaf expansion might be the result of N reallocation independent from leaf senescence. Second, leaf growth is the result of two uncoupled developmental processes: cell expansion and cell division (Tsiantis & Hay, 2003). Cell expansion is mainly constrained by water availability while cell division depends on photosynthates (Körner, 2013), suggesting that leaf growth can still occur during senescence in well-watered conditions despite the drop of carbon assimilation. Moreover, leaf DM still increased after the decline of leaf expansion and LNC in our dataset, consistently with the late increase in sugar concentration observed in several *A. thaliana* recombinant inbred lines (Diaz et al., 2005). These observations challenge our conception of leaf nitrogen and carbon in- and outfluxes during leaf ageing. Our study was limited to tracking a single leaf per plant and during the second half of its life span. Dedicated studies are needed to better understand how the dynamics of leaf properties are driven by plant life-history events such as the production of new leaves and reproductive organs.

Given its importance for plant resource economics, nitrogen acquisition and conservation strategies have been included in a slow–fast syndrome at both plant and leaf levels (Reich, 2014). However, previous interspecific explorations of the linkage between resorption efficiency and leaf economics traits did not report clear signals (Freschet et al., 2010; Kazakou et al., 2007). As expected, our results showed that high resorption efficiency was associated with low SLA and late maturity corresponding to a slow-leaf and slow-plant syndromes (Sartori et al., 2019) respectively. Conversely, fast syndromes were characterized by low resorption efficiency. However, correlations were weak, indicating that for a given value of resorption efficiency, plants expressed a large range of SLA and FT values. By contrast, we observed a narrower correlation between resorption rate and plant and leaf syndromes in our dataset. The fact that slow strategies at the plant and leaf level were characterized by high leaf resorption rates contradicts our initial expectations. Leaves from fast-growing plants exhibited a slow decrease in nitrogen quantity while leaves from slow-growing plants had fast nitrogen resorption within a short time. Fast-growing genotypes reach sexual maturity earlier with a lower plant biomass and leaf number than slow-growing genotypes (Vasseur et al., 2012), consistent with a slow–fast syndrome (Dammhahn et al., 2018; Salguero-Gómez et al., 2016). Thus, the leaf resorption rate of nitrogen might be adjusted to the plant-level nitrogen demand. As reported by Diaz et al. (2005), the time course of leaf senescence is correlated with the total number of leaves that compose the rosette in *A. thaliana*. According to Harper and Sellek (1987), the main driver of nitrogen resorption is the strength of the nitrogen demand from newly formed leaves. We thus hypothesize that large plants composed of numerous leaves impose a strong nitrogen demand on senescent leaves. In addition, as we measured traits after bolting and on plants growing in low nitrogen conditions, the construction of reproductive organs may impose a supplementary nitrogen demand on leaves (Havé et al., 2017; Masclaux-Daubresse & Chardon, 2011). This strong source–sink relationship suggests that leaf-level resorption capacity can be uncoupled from leaf-level resource-use strategies and should be considered relative to whole-plant functioning. This is consistent with recent studies showing that leaf economics and resorption capacities are influenced by whole-plant functioning (Rea et al., 2018; Sartori et al., 2019). Future experimental studies measuring nitrogen transfers between organs of the whole individuals are needed to properly test these assumptions. Moreover, the timing and the intensity of the nitrogen demand, and the role of the demand itself that a leaf experiences, might be of different importance depending on the species, especially in woody, long-lived and evergreen species.

Our results did not show any correlation between nitrogen resorption efficiency or rate, and precipitations, contrary to previous observations in interspecific biogeographic meta-analyses (Drenovsky et al., 2019; Yuan & Chen, 2009). Given that resorption efficiency is known to vary depending on the growing conditions (Chapin, 1980), phenotypic plasticity could also be responsible for the lack of relationship in our dataset. The effect of water availability on the resorption capacity could be mediated through phenotypic plasticity, rather than local adaptation, and growing plants in homogeneous conditions would have removed such influence of phenotypic plasticity. By contrast, the rate and efficiency of nitrogen resorption covaried with climate: High rates and efficiency of nitrogen resorption were expressed by genotypes originating from cooler habitats. Despite the importance of microclimate for *A. thaliana* local adaptation (Brachi et al., 2013), annual temperature may reflect the average growing conditions that the populations encounter. Therefore, environmental variables capturing spatially imprecise data are still considered approximate estimators of stress that plants experience (Borgy et al., 2017). The relatively recent migration of *A. thaliana* towards Scandinavia was accompanied by allele fixation conferring resistance to harsh environmental conditions imposed by

coldness (Exposito-Alonso et al., 2018; Krämer, 2015). Such climatic constraints should have selected for trait values characteristic of a conservative syndrome (Borgy et al., 2017), such as low LES scores (Sartori et al., 2019), and trait values determinant for leaf senescence and life span such as resorption rate and efficiency. However, it will be important to account for variation in local soil resource availability to further explore the biogeographical determinants of the different facets of resorption ability (Drenovsky et al., 2019). Indeed, nutrient-poor environments are supposed to select for traits reducing nutrient losses (Aerts & Chapin, 1999) and thus, should also regulate the variation in nutrient resorption rate.

The highest heritability the resorption rate of nitrogen was reflected by the numerous genetic associations detected along the *A. thaliana* genome. While, in this study, our ambition was not to identify genes that are determinant for the resorption capacity in *A. thaliana*, one locus was of particular interest. The ATCCS gene was significantly associated with the resorption rate of nitrogen. Our genetic analysis informs that one ATCCS' allele, associated with high resorption rate, is favoured at high latitudes and low temperatures, while the reverse syndrome is associated with the second allele. Moreover, the F_{ST} analysis demonstrates that the genetic differentiation between *A. thaliana* populations at this specific locus is high, suggesting that disruptive selection maintains diversity responding to geographical and environmental gradients. The ATCCS gene is involved in a cellular mechanism that detoxifies superoxide radicals (Sun et al., 2017). Protecting leaves against photo-oxidative stress is of particular concern for plants growing at cold temperatures, since the photosynthetic capacity decreases while the light is still abundant (Ougham et al., 2008). Protecting leaves that are already senescing might not be of critical importance (Pena-Novas & Archetti, 2021). Yet, the photoprotection hypothesis, initially developed in tree ecology, suggests that the adaptive value of oxidative stress reducers is to maintain leaves' functioning during senescence and improve nutrient resorption at low temperature, and in particular nitrogen resorption (Feild & Brodribb, 2013; Hoch et al., 2003; Lee et al., 2003; Pena-Novas & Archetti, 2021). This result is a rare convergence between genomic and ecological findings. It demonstrates the role of nitrogen resorption in leaf senescence and life span, and its importance for local adaptation. Copper chaperones were already associated with the resorption efficiency in *A. thaliana*, using a set of mutants from the genotype Wassilewskija background (Himelblau & Amasino, 2001). It questions how and why we were able to detect ATCCS through the resorption rate's GWAs, while the resorption efficiency GWAs was unsuccessful. First of all, artificial mutations as performed by Himelblau & Amasino might have drastic effects such as gene knockout, and strongly influence the resorption process as a whole. By contrast, punctual natural mutations might have a moderate effect, adjusting the resorption process to the environmental constraints. We hypothesize that, by protecting the leaves against photo-oxidation, the copper chaperones allow a fast nitrogen resorption in controlled conditions, while it guarantees a fulfilling resorption efficiency in stressful conditions.

Overall, our results emphasize the ecological and evolutionary importance of a leaf nitrogen resorption component that has been poorly explored so far. Combined with genetic and climatic data, our findings reveal that high resorption rates of nitrogen, rather than high resorption efficiency, are favoured towards the northern and colder region of the *A. thaliana* distribution. We provide evidence that the resorption rate is integrated in leaf and plant level resource-use strategies and growth syndrome, suggesting its importance for better plant fitness characterization. Next steps will be to explore the anatomical and molecular determinants of the resorption rate as done for nitrogen resorption efficiency, such as the leaf vein architecture (Zhang et al., 2015) and the enzymes responsible for N-bearing molecule catalysis and transport (Moison et al., 2018). Finally, future studies might also explore the relative role of soil nitrogen availability and plant nitrogen demand on the time course of nitrogen at the organ and plant levels. The combined use of comparative ecology, quantitative genetics and population genetics is a promising avenue to understand the role of physiological constraints and trait syndromes in plant adaptation.

ACKNOWLEDGEMENTS

We are grateful to Thierry Mathieu, David Degueldre, and Pauline Durbin from the TE platform of the Labec CEMEB for their technical assistance. We also thank Pascal Tillard for his assistance with CHN measurements. This work was supported by the European Research Council (ERC; ERC-StG-2014-639706-CONSTRAINTS grant).

CONFLICT OF INTEREST

We declare no conflicts of interest. Cyrille Violle is an Associate Editor of Functional Ecology, but took no part in the peer review and decision-making processes for this paper.

AUTHORS' CONTRIBUTIONS

K.S., E.K., D.V. and C.V. conceived the ideas and designed methodology; K.S., L.G. and L.R.F. collected the data; K.S., F.V., P.d.V., J.B. analyzed the data; K.S., C.V., D.V. and E.K. led the writing of the manuscript. All authors contributed critically to the drafts and gave final approval for publication.

DATA AVAILABILITY STATEMENT

Data available from the Zenodo repository: https://doi.org/10.5281/zenodo.6140504 (Sartori et al., 2022).

ORCID

Kevin Sartori https://orcid.org/0000-0001-7364-1341
Cyrille Violle https://orcid.org/0000-0002-2471-9226
Denis Vile https://orcid.org/0000-0002-7948-1462
François Vasseur https://orcid.org/0000-0002-0575-6216
Pierre de Villemereuil https://orcid.org/0000-0002-8791-6104
Lauren Gillespie https://orcid.org/0000-0002-2294-4411
Elena Kazakou https://orcid.org/0000-0001-7188-8367

REFERENCES

Achat, D. L., Pousse, N., Nicolas, M., & Augusto, L. (2018). Nutrient remobilization in tree foliage as affected by soil nutrients and leaf life span. *Ecological Monographs*, *88*(3), 408–428. https://doi.org/10.1002/ecm.1300

Aerts, R., & Chapin, F. S. (1999). The mineral nutrition of wild plants revisited: A re-evaluation of processes and patterns. In A. H. Fitter & D. G. Raffaelli (Eds.), *Advances in ecological research* (Vol. *30*, pp. 1–67). Academic Press. https://doi.org/10.1016/S0065-2504(08)60016-1

Agrawal, A. A. (2020). A scale-dependent framework for trade-offs, syndromes, and specialization in organismal biology. *Ecology*, *101*(2), e02924. https://doi.org/10.1002/ecy.2924

Alonso-Blanco, C., Andrade, J., Becker, C., Bemm, F., Bergelson, J., Borgwardt, K. M., Cao, J., Chae, E., Dezwaan, T. M., Ding, W., Ecker, J. R., Exposito-Alonso, M., Farlow, A., Fitz, J., Gan, X., Grimm, D. G., Hancock, A. M., Henz, S. R., Holm, S., … Zhou, X. (2016). 1,135 genomes reveal the global pattern of polymorphism in *Arabidopsis thaliana*. *Cell*, *166*(2), 481–491. https://doi.org/10.1016/j.cell.2016.05.063

Baraloto, C., Paine, C. E. T., Patiño, S., Bonal, D., Hérault, B., & Chave, J. (2010). Functional trait variation and sampling strategies in species-rich plant communities. *Functional Ecology*, *24*(1), 208–216. https://doi.org/10.1111/j.1365-2435.2009.01600.x

Berardini, T. Z., Reiser, L., Li, D., Mezheritsky, Y., Muller, R., Strait, E., & Huala, E. (2015). The arabidopsis information resource: Making and mining the "gold standard" annotated reference plant genome. *Genesis*, *53*(8), 474–485. https://doi.org/10.1002/dvg.22877

Berendse, F., & Aerts, R. (1987). Nitrogen-use-efficiency: A biologically meaningful definition? *Functional Ecology*, *1*(3), 293–296.

Bloom, A. J., Chapin, F. S., & Mooney, H. A. (1985). Resource limitation in plants—An economic analogy. *Annual Review of Ecology and Systematics*, *16*(1), 363–392. https://doi.org/10.1146/annurev.es.16.110185.002051

Bonhomme, M., Fariello, M. I., Navier, H., Hajri, A., Badis, Y., Miteul, H., Samac, D. A., Dumas, B., Baranger, A., Jacquet, C., & Pilet-Nayel, M.-L. (2019). A local score approach improves GWAS resolution and detects minor QTL: application to Medicago truncatula quantitative disease resistance to multiple Aphanomyces euteiches isolates. *Heredity*, *123*(4), 517–531. https://doi.org/10.1038/s41437-019-0235-x

Borgy, B., Violle, C., Choler, P., Denelle, P., Munoz, F., Kattge, J., Lavorel, S., Loranger, J., Amiaud, B., Bahn, M., van Bodegom, P. M., Brisse, H., Debarros, G., Diquelou, S., Gachet, S., Jolivet, C., Lemauviel-Lavenant, S., Mikolajczak, A., Olivier, J., … Garnier, E. (2017). Plant community structure and nitrogen inputs modulate the climate signal on leaf traits. *Global Ecology and Biogeography*, *26*(10), 1138–1152. https://doi.org/10.1111/geb.12623

Brachi, B., Aimé, C., Glorieux, C., Cuguen, J., & Roux, F. (2012). Adaptive value of phenological traits in stressful environments: Predictions based on seed production and laboratory natural selection. *PLoS One*, *7*(3), e32069. https://doi.org/10.1371/journal.pone.0032069

Brachi, B., Villoutreix, R., Faure, N., Hautekèete, N., Piquot, Y., Pauwels, M., Roby, D., Cuguen, J., Bergelson, J., & Roux, F. (2013). Investigation of the geographical scale of adaptive phenological variation and its underlying genetics in *Arabidopsis thaliana*. *Molecular Ecology*, *22*(16), 4222–4240. https://doi.org/10.1111/mec.12396

Campanella, M. V., & Bertiller, M. B. (2011). Is N-resorption efficiency related to secondary compounds and leaf longevity in coexisting plant species of the arid Patagonian Monte, Argentina? *Austral Ecology*, *36*(4), 395–402. https://doi.org/10.1111/j.1442-9993.2010.02165.x

Chapin, F. S. (1980). The mineral nutrition of wild plants. *Annual Review of Ecology and Systematics*, *11*(1), 233–260. https://doi.org/10.1146/annurev.es.11.110180.001313

Chave, J., Coomes, D., Jansen, S., Lewis, S. L., Swenson, N. G., & Zanne, A. E. (2009). Towards a worldwide wood economics spectrum. *Ecology Letters*, *12*(4), 351–366. https://doi.org/10.1111/j.1461-0248.2009.01285.x

Dammhahn, M., Dingemanse, N. J., Niemelä, P. T., & Réale, D. (2018). Pace-of-life syndromes: A framework for the adaptive integration of behaviour, physiology and life history. *Behavioral Ecology and Sociobiology*, *72*(3). https://doi.org/10.1007/s00265-018-2473-y

Danecek, P., Auton, A., Abecasis, G., Albers, C. A., Banks, E., DePristo, M. A., Handsaker, R. E., Lunter, G., Marth, G. T., Sherry, S. T., McVean, G., & Durbin, R.; 1000 Genomes Project Analysis Group. (2011). The variant call format and VCFtools. *Bioinformatics*, *27*(15), 2156–2158. https://doi.org/10.1093/bioinformatics/btr330

DeLeo, V. L., Menge, D. N. L., Hanks, E. M., Juenger, T. E., & Lasky, J. R. (2020). Effects of two centuries of global environmental variation on phenology and physiology of *Arabidopsis thaliana*. *Global Change Biology*, *26*(2), 523–538. https://doi.org/10.1111/gcb.14880

Diaz, C., Lemaître, T., Christ, A., Azzopardi, M., Kato, Y., Sato, F., Morot-Gaudry, J.-F., Dily, F. L., & Masclaux-Daubresse, C. (2008). Nitrogen recycling and remobilization are differentially controlled by leaf senescence and development stage in Arabidopsis under low nitrogen nutrition. *Plant Physiology*, *147*(3), 1437–1449. https://doi.org/10.1104/pp.108.119040

Diaz, C., Purdy, S., Christ, A., Morot-Gaudry, J.-F., Wingler, A., & Masclaux-Daubresse, C. (2005). Characterization of markers to determine the extent and variability of leaf senescence in Arabidopsis. A metabolic profiling approach. *Plant Physiology*, *138*(2), 898–908. https://doi.org/10.1104/pp.105.060764

Drenovsky, R. E., Pietrasiak, N., & Short, T. H. (2019). Global temporal patterns in plant nutrient resorption plasticity. *Global Ecology and Biogeography*, *28*(6), 728–743. https://doi.org/10.1111/geb.12885

Ecarnot, M., Compan, F., & Roumet, P. (2013). Assessing leaf nitrogen content and leaf mass per unit area of wheat in the field throughout plant cycle with a portable spectrometer. *Field Crops Research*, *140*, 44–50. https://doi.org/10.1016/j.fcr.2012.10.013

Exposito-Alonso, M., Vasseur, F., Ding, W., Wang, G., Burbano, H. A., & Weigel, D. (2018). Genomic basis and evolutionary potential for extreme drought adaptation in *Arabidopsis thaliana*. *Nature Ecology & Evolution*, *2*(2), 352–358. https://doi.org/10.1038/s41559-017-0423-0

Feild, T. S., & Brodribb, T. J. (2013). Hydraulic tuning of vein cell microstructure in the evolution of angiosperm venation networks. *New Phytologist*, *199*(3), 720–726. https://doi.org/10.1111/nph.12311

Freschet, G. T., Cornelissen, J. H. C., van Logtestijn, R. S. P., & Aerts, R. (2010). Substantial nutrient resorption from leaves, stems and roots in a subarctic flora: What is the link with other resource economics traits? *New Phytologist*, *186*(4), 879–889. https://doi.org/10.1111/j.1469-8137.2010.03228.x

Genolini, C., Ecochard, R., Benghezal, M., Driss, T., Andrieu, S., & Subtil, F. (2016). kmlShape: An efficient method to cluster longitudinal data (time-series) according to their shapes. *PLoS One*, *11*(6), e0150738. https://doi.org/10.1371/journal.pone.0150738

Harper, J. L., & Sellek, C. (1987). The effects of severe mineral nutrient deficiencies on the demography of leaves. *Proceedings of the Royal Society of London. Series B. Biological Sciences*, *232*(1267), 137–157. https://doi.org/10.1098/rspb.1987.0065

Havé, M., Marmagne, A., Chardon, F., & Masclaux-Daubresse, C. (2017). Nitrogen remobilization during leaf senescence: Lessons from Arabidopsis to crops. *Journal of Experimental Botany*, *68*(10), 2513–2529. https://doi.org/10.1093/jxb/erw365

Heerwaarden, L. M. V., Toet, S., & Aerts, R. (2003). Current measures of nutrient resorption efficiency lead to a substantial underestimation of real resorption efficiency: Facts and solutions. *Oikos*, *101*(3), 664–669. https://doi.org/10.1034/j.1600-0706.2003.12351.x

Himelblau, E., & Amasino, R. M. (2001). Nutrients mobilized from leaves of *Arabidopsis thaliana* during leaf senescence. *Journal of Plant Physiology*, *158*(10), 1317–1323. https://doi.org/10.1078/0176-1617-00608

Hoch, W. A., Singsaas, E. L., & McCown, B. H. (2003). Resorption protection. Anthocyanins facilitate nutrient recovery in autumn by shielding leaves from potentially damaging light levels. *Plant Physiology*, *133*(3), 1296–1305. https://doi.org/10.1104/pp.103.027631

Isaac, M. E., Martin, A. R., de Melo Virginio Filho, E., Rapidel, B., Roupsard, O., & Van den Meersche, K. (2017). Intraspecific trait variation and coordination: Root and leaf economics spectra in coffee across environmental gradients. *Frontiers in Plant Science*, *8*. https://doi.org/10.3389/fpls.2017.01196

Kazakou, E., Garnier, E., Navas, M.-L., Roumet, C., Collin, C., & Laurent, G. (2007). Components of nutrient residence time and the leaf economics spectrum in species from Mediterranean old-fields differing in successional status. *Functional Ecology*, *21*(2), 235–245. https://doi.org/10.1111/j.1365-2435.2006.01242.x

Killingbeck, K. T. (1986). The terminological jungle revisited: Making a case for use of the term resorption. *Oikos*, *46*(2), 263. https://doi.org/10.2307/3565477

Kim, S. (2015). ppcor: An R package for a fast calculation to semi-partial correlation coefficients. *Communications for Statistical Applications and Methods*, *22*(6), 665–674. https://doi.org/10.5351/CSAM.2015.22.6.665

Körner, C. (2013). Growth controls photosynthesis—Mostly. *Nova Acta Leopoldina*, *114*(391), 273–283. https://doi.org/10.1007/s00442-012-2371

Krämer, U. (2015). Planting molecular functions in an ecological context with *Arabidopsis thaliana*. *elife*, *4*, e06100. https://doi.org/10.7554/eLife.06100

Lasky, J. R., Des Marais, D. L., McKAY, J. K., Richards, J. H., Juenger, T. E., & Keitt, T. H. (2012). Characterizing genomic variation of *Arabidopsis thaliana*: The roles of geography and climate: Geography, climate and Arabidopsis genomics. *Molecular Ecology*, *21*(22), 5512–5529. https://doi.org/10.1111/j.1365-294X.2012.05709.x

Lee, D. W., O'Keefe, J., Holbrook, N. M., & Feild, T. S. (2003). Pigment dynamics and autumn leaf senescence in a New England deciduous forest, eastern USA. *Ecological Research*, *18*(6), 677–694. https://doi.org/10.1111/j.1440-1703.2003.00588.x

Lesnoff, M., Metz, M., & Roger, J.-M. (2020). Comparison of locally weighted PLS strategies for regression and discrimination on agronomic NIR data. *Journal of Chemometrics*, *34*(5), e3209. https://doi.org/10.1002/cem.3209

Lovell, J. T., Juenger, T. E., Michaels, S. D., Lasky, J. R., Platt, A., Richards, J. H., Yu, X., Easlon, H. M., Sen, S., & McKay, J. K. (2013). Pleiotropy of FRIGIDA enhances the potential for multivariate adaptation. *Proceedings of the Royal Society of London B: Biological Sciences*, *280*(1763), 20131043. https://doi.org/10.1098/rspb.2013.1043

Masclaux-Daubresse, C., & Chardon, F. (2011). Exploring nitrogen remobilization for seed filling using natural variation in Arabidopsis thaliana. *Journal of Experimental Botany*, *62*(6), 2131–2142. https://doi.org/10.1093/jxb/erq405

Mendez-Vigo, B., Pico, F. X., Ramiro, M., Martinez-Zapater, J. M., & Alonso-Blanco, C. (2011). Altitudinal and climatic adaptation is mediated by flowering traits and FRI, FLC, and PHYC genes in Arabidopsis. *Plant Physiology*, *157*(4), 1942–1955. https://doi.org/10.1104/pp.111.183426

Mikola, J., Silfver, T., Paaso, U., Possen, B. J. M. H., & Rousi, M. (2018). Leaf N resorption efficiency and litter N mineralization rate have a genotypic tradeoff in a silver birch population. *Ecology*, *99*(5), 1227–1235. https://doi.org/10.1002/ecy.2176

Mitchell-Olds, T. (2001). Arabidopsis thaliana and its wild relatives: A model system for ecology and evolution. *Trends in Ecology & Evolution*, *16*(12), 693–700. https://doi.org/10.1016/S0169-5347(01)02291-1

Moison, M., Marmagne, A., Dinant, S., Soulay, F., Azzopardi, M., Lothier, J., Citerne, S., Morin, H., Legay, N., Chardon, F., Avice, J.-C., Reisdorf-Cren, M., & Masclaux-Daubresse, C. (2018). Three cytosolic glutamine synthetase isoforms localized in different-order veins act together for N remobilization and seed filling in Arabidopsis. *Journal of Experimental Botany*, *69*(18), 4379–4393. https://doi.org/10.1093/jxb/ery217

Niinemets, U., & Tamm, U. (2005). Species differences in timing of leaf fall and foliage chemistry modify nutrient resorption efficiency in deciduous temperate forest stands. *Tree Physiology*. https://doi.org/10.1093/TREEPHYS/25.8.1001

Osaki, M., & Shinano, T. (2001). Plant growth based on interrelation between carbon and nitrogen translocation from leaves. *Photosynthetica*, *39*(2), 197–203. https://doi.org/10.1023/A:1013770807583

Ougham, H., Hörtensteiner, S., Armstead, I., Donnison, I., King, I., Thomas, H., & Mur, L. (2008). The control of chlorophyll catabolism and the status of yellowing as a biomarker of leaf senescence. *Plant Biology*, *10*(Suppl. 1), 4–14. https://doi.org/10.1111/j.1438-8677.2008.00081.x

Pantin, F., Simonneau, T., & Muller, B. (2012). Coming of leaf age: Control of growth by hydraulics and metabolics during leaf ontogeny. *New Phytologist*, *196*(2), 349–366. https://doi.org/10.1111/j.1469-8137.2012.04273.x

Pena-Novas, I., & Archetti, M. (2021). A test of the photoprotection hypothesis for the evolution of autumn colours: Chlorophyll resorption, not anthocyanin production, is correlated with nitrogen translocation. *Journal of Evolutionary Biology*, *34*(9), 1423–1431. https://doi.org/10.1111/jeb.13903

Purcell, S., Neale, B., Todd-Brown, K., Thomas, L., Ferreira, M. A. R., Bender, D., Maller, J., Sklar, P., de Bakker, P. I. W., Daly, M. J., & Sham, P. C. (2007). PLINK: A tool set for whole-genome association and population-based linkage analyses. *The American Journal of Human Genetics*, *81*(3), 559–575. https://doi.org/10.1086/519795

R Core Team. (2019). *R: A Language and Environment for Statistical Computing*. R Foundation for Statistical Computing. https://www.R-project.org/

Rea, A. M., Mason, C. M., & Donovan, L. A. (2018). Evolution of nutrient resorption across the herbaceous genus Helianthus. *Plant Ecology*, *219*(8), 887–899. https://doi.org/10.1007/s11258-018-0841-3

Reich, P. B. (2014). The world-wide 'fast–slow' plant economics spectrum: A traits manifesto. *Journal of Ecology*, *102*(2), 275–301. https://doi.org/10.1111/1365-2745.12211

Reich, P. B., Walters, M. B., & Ellsworth, D. S. (1991). Leaf age and season influence the relationships between leaf nitrogen, leaf mass per area and photosynthesis in maple and oak trees. *Plant, Cell & Environment*, *14*(3), 251–259. https://doi.org/10.1111/j.1365-3040.1991.tb01499.x

Salguero-Gómez, R. (2017). Applications of the fast-slow continuum and reproductive strategy framework of plant life histories. *New Phytologist*, *213*(4), 1618–1624. https://doi.org/10.1111/nph.14289

Salguero-Gómez, R., Jones, O. R., Jongejans, E., Blomberg, S. P., Hodgson, D. J., Mbeau-Ache, C., Zuidema, P. A., de Kroon, H., & Buckley, Y. M. (2016). Fast–slow continuum and reproductive strategies structure plant life-history variation worldwide. *Proceedings of the National Academy of Sciences of the United States of America*, *113*(1), 230–235. https://doi.org/10.1073/pnas.1506215112

Santiago, J. P., & Tegeder, M. (2017). Implications of nitrogen phloem loading for carbon metabolism and transport during Arabidopsis development. *Journal of Integrative Plant Biology*, *59*(6), 409–421. https://doi.org/10.1111/jipb.12533

Sartori, K., Vasseur, F., Violle, C., Baron, E., Gerard, M., Rowe, N., Ayala-Garay, O., Christophe, A., Jalón, L. G. D., Masclef, D., Harscouet, E., Granado, M. D. R., Chassagneux, A., Kazakou, E., & Vile, D. (2019). Leaf economics and slow-fast adaptation across the geographic range of *Arabidopsis thaliana*. *Scientific Reports*, *9*(1), 10758. https://doi.org/10.1038/s41598-019-46878-2

Sartori, K., Violle, C., Vile, D., Vasseur, F., de Villemereuil, P., Bresson, J., Gillespie, L., Fletcher, L. R., Sack, L., & Kazakou, E. (2022).

Nitrogen resorption dynamics and slow-fast strategies in 137 *Arabidopsis thaliana* genotypes. *Zenodo*, https://doi.org/10.5281/zenodo.6140505

Schmalenbach, I., Zhang, L., Ryngajllo, M., & Jiménez-Gómez, J. M. (2014). Functional analysis of the *Landsberg erecta* allele of FRIGIDA. *BMC Plant Biology*, *14*(1), 1. https://doi.org/10.1186/s12870-014-0218-2

Schneider, C. A., Rasband, W. S., & Eliceiri, K. W. (2012). NIH image to ImageJ: 25 years of image analysis. *Nature Methods*, *9*(7), 671–675. https://doi.org/10.1038/nmeth.2089

Searle, S. R., Speed, F. M., & Milliken, G. A. (1980). Population marginal means in the linear model: An alternative to least squares means. *The American Statistician*, *34*(4), 216–221. https://doi.org/10.1080/00031305.1980.10483031

Sun, Y., Wang, Y., Wang, G., Xiang, L., & Qi, J. (2017). A new anti-aging lysophosphatidic acid from *Arabidopsis thaliana*. *Medicinal Chemistry*, *13*(7), 641–647. https://doi.org/10.2174/1573406413666170209124934

Tjoelker, M. G., Craine, J. M., Wedin, D., Reich, P. B., & Tilman, D. (2005). Linking leaf and root trait syndromes among 39 grassland and savannah species. *New Phytologist*, *167*(2), 493–508. https://doi.org/10.1111/j.1469-8137.2005.01428.x

Tsiantis, M., & Hay, A. (2003). Comparative plant development: The time of the leaf? *Nature Reviews Genetics*, *4*(3), 169–180. https://doi.org/10.1038/nrg1002

Vasseur, F., Sartori, K., Baron, E., Fort, F., Kazakou, E., Segrestin, J., Garnier, E., Vile, D., & Violle, C. (2018). Climate as a driver of adaptive variations in ecological strategies in *Arabidopsis thaliana*. *Annals of Botany*, *122*(6), 935–945. https://doi.org/10.1093/aob/mcy165

Vasseur, F., Violle, C., Enquist, B. J., Granier, C., & Vile, D. (2012). A common genetic basis to the origin of the leaf economics spectrum and metabolic scaling allometry. *Ecology Letters*, *15*(10), 1149–1157. https://doi.org/10.1111/j.1461-0248.2012.01839.x

Vilmus, I., Ecarnot, M., Verzelen, N., & Roumet, P. (2014). Monitoring nitrogen leaf resorption kinetics by near-infrared spectroscopy during grain filling in durum wheat in different nitrogen availability conditions. *Crop Science*, *54*(1), 284–296. https://doi.org/10.2135/cropsci2013.02.0099

Weir, B. S., & Cockerham, C. C. (1984). Estimating *F*-statistics for the analysis of population structure. *Evolution*, *38*(6), 1358–1370. https://doi.org/10.1111/j.1558-5646.1984.tb05657.x

Whitfield, R. G., Gerger, M. E., & Sharp, R. L. (1987). Near-infrared spectrum qualification via Mahalanobis distance determination. *Applied Spectroscopy*, *41*(7), 1204–1213. https://doi.org/10.1366/0003702874447572

Withington, J. M., Reich, P. B., Oleksyn, J., & Eissenstat, D. M. (2006). Comparisons of structure and life span in roots and leaves among temperate trees. *Ecological Monographs*, *76*(3), 381–397. https://doi.org/10.1890/0012-9615(2006)076[0381:COSALS]2.0.CO;2

Wright, I. J., Reich, P. B., Westoby, M., Ackerly, D. D., Baruch, Z., Bongers, F., Cavender-Bares, J., Chapin, T., Cornelissen, J. H. C., Diemer, M., Flexas, J., Garnier, E., Groom, P. K., Gulias, J., Hikosaka, K., Lamont, B. B., Lee, T., Lee, W., Lusk, C., … Villar, R. (2004). The worldwide leaf economics spectrum. *Nature*, *428*(6985), 821–827. https://doi.org/10.1038/nature02403

Yuan, Z. Y., & Chen, H. Y. H. (2009). Global-scale patterns of nutrient resorption associated with latitude, temperature and precipitation. *Global Ecology and Biogeography*, *18*(1), 11–18. https://doi.org/10.1111/j.1466-8238.2008.00425.x

Yuan, Z. Y., & Chen, H. Y. H. (2010). Changes in nitrogen resorption of trembling aspen (*Populus tremuloides*) with stand development. *Plant and Soil*, *327*(1), 121–129. https://doi.org/10.1007/s11104-009-0036-8

Zavala-Ortiz, D. A., Ebel, B., Li, M.-Y., Barradas-Dermitz, D. M., Hayward-Jones, P. M., Aguilar-Uscanga, M. G., Marc, A., & Guedon, E. (2020). Interest of locally weighted regression to overcome nonlinear effects during in situ NIR monitoring of CHO cell culture parameters and antibody glycosylation. *Biotechnology Progress*, *36*(1), e2924. https://doi.org/10.1002/btpr.2924

Zhang, J.-L., Zhang, S.-B., Chen, Y.-J., Zhang, Y.-P., & Poorter, L. (2015). Nutrient resorption is associated with leaf vein density and growth performance of dipterocarp tree species. *Journal of Ecology*, *103*(3), 541–549. https://doi.org/10.1111/1365-2745.12392

Zhou, X., Carbonetto, P., & Stephens, M. (2013). Polygenic modeling with bayesian sparse linear mixed models. *PLoS Genetics*, *9*(2), e1003264. https://doi.org/10.1371/journal.pgen.1003264

Zhou, X., & Stephens, M. (2012). Genome-wide efficient mixed-model analysis for association studies. *Nature Genetics*, *44*(7), 821–824. https://doi.org/10.1038/ng.2310

SUPPORTING INFORMATION

Additional supporting information may be found in the online version of the article at the publisher's website.

How to cite this article: Sartori, K., Violle, C., Vile, D., Vasseur, F., de Villemereuil, P., Bresson, J., Gillespie, L., Fletcher, L. R., Sack, L., & Kazakou, E. (2022). Do leaf nitrogen resorption dynamics align with the slow-fast continuum? A test at the intraspecific level. *Functional Ecology*, *36*, 1315–1328. https://doi.org/10.1111/1365-2435.14029